ACADEMY OF SCIENCES OF KAZAKH SSR

FERMILAB-PUB-78-135-E

HIGH ENERGY PHYSICS INSTITUTE

Preprint

HEPI 67 - 78

INVESTIGATION OF INELASTIC INTERACTIONS OF 400 GEV PROTONS WITH EMULSION NUCLEI

Alma-Ata-Gatchina-Moscow-Tashkent

Collaboration

RECEIVED
SEP 12 1978
DIRECTORS OFFICE
FERMILAB

Alma-Ata 1978

FERMILAB-PUB-78-135-E

Experiment 463

Submitted to XIX International Conference on High Energy Physics and Nucl. Physics B.

ACADEMY OF SCIENCES OF KAZAKH SSR

HIGH ENERGY PHYSICS INSTITUTE

Preprint

HEPI 67 - 78

INVESTIGATION OF INELASTIC INTERACTIONS OF 400 GEV PROTONS WITH EMULSION NUCLEI

Alma-Ata - Gatchina - Moscow - Tashkent Collaboration

E.G.Boos, A.I.Borisenko*, A.N.Kazanskaya*, A.V.Kholmetskaya, P.V.Morozova* and N.P.Pavlova

Institute for High Energy Physics of Kazakh Academy of Sciences, Alma-Ata, USSR

F.G.Lepekhin and B.B.Simonov

Leningrad Institute of Nuclear Physics of Soviet Academy of Sciences, Gatchina, USSR

M.I.Adamovich, M.M.Chernyavskij, S.P.Kharlamov, V.G. Larionova, N.V.Maslennikova, G.I.Orlova, M.I.Tretyakova and F.R.Yagudina

P.N.Lebedev Physical Institute of Soviet Academy of Sciences, Moscow, USSR

Sh.Abduzhamilov, S.A.Azimov, L.P.Chernova, G.M.Chernov, S.I.Gadzhieva, K.G.Gulamov, Kh.D.Kabulniyazov, N.S.Kasymova, V.I.Petrov, N.S.Scripnik and T.P.Trofimova**

S.V.Starodubtsev Physical Technical Institute of Uzbek Academy of Sciences, Tashkent, USSR

---

*Permanent address: S.M.Kirov Kazakh State University, Alma-Ata

**Presently at Institute of Nuclear Physics of Uzbek Academy of Sciences, Ulugbek, Tashkent 702132, USSR

ABSTRACT

The basic experimental characteristics of incoherent interactions of 400 Gev protons on emulsion nuclei, such as multiplicity of charged secondaries, one-particle distributions and two-particle correlations, are reported and discussed in detail. They are compared with results of other experiments on hadron-nucleus interactions of more low energies. We have shown from the comparison, both qualitative and quantitative, of the data presented with predictions of various model approaches suggested recently for nuclear production that most of cannot explain the complete set of experimental observations.

An analysis of the experimental data obtained, gives strong support to the idea that the production mechanism in hadron-nucleus interactions has two- or multicomponent character.

FERMILAB-PUB-78-135-E

© Институт физики высоких энергий Академии наук Казахской ССР, 1978.

Отпечатано на ротапринте Института физики высоких энергий Академии наук Казахской ССР.
Заказ № 606. Уч.-изд. листов 2,3. Тираж 150 экз.

Печатается по постановлению Ученого совета ИФВЭ АН КазССР. Ответственный за выпуск к.ф.-м.н. Н.П.Павлова.

УДК 539.12

1. Introduction

There has been a growing interest in the study of high-energy hadron-nucleus interactions in recent years, based on the idea of the possible use of a nucleus as an analyser of the space-time structure of multiple production to discriminate between various theoretical approaches. Although a considerable effort , both experimental and theoretical, has already been devoted to the understanding of nuclear production, it should be emphasizad that the accumulation of accurate experimental data is still a current problem.

This work is one in a series of emulsion experiments on hadron-nucleus (hA) interactions performed by our collaboration in the Fermilab energy range and it is concerned with the analysis of various characteristics, such as multiplicity of charged secondaries, angular distributions and correlations, in inelastic proton-nucleus interactions at 400 GeV. Also, we shall consider here the energy dependence of some basic characteristics of hA collisions using experimental data on pA and π^-A collisions at lower ener-

gies available with us, and a comparison, both qualitative and quantitative, will be performed of these data with predictions of some popular models suggested recently for production on nuclei.

Our paper is organized as follows. Section 2 describes the experimental material used. Sections 3-5 contain multiplicity, one-particle distributions and two-particle correlations, respectively. Finally, in section 6 we briefly summarize the results of our investigation.

Before discussing the data, it is useful to note that earlier we published in preprint form [1] some preliminary results based on a small amount of the present statistic .

2. Experimental material

Stacks of GOSNIIHIMFOTOPROEK BR-2 emulsion, each containing pellicles of dimensions 10cm x 20cm x 600 μm, were exposed to the 400 GeV proton beam at the Fermi National Accelerator Laboratory. The beam flux was chosen to be $(2 \div 4) \cdot 10^4$ protons/cm^2. By along-the-track scanning, which has been in part performed doubly, 3628 inelastic events were recorded without any discrimination along the total effective length of 1269 m , leading to the mean free path for inelastic interaction in emulsion $\lambda = (35.0 \pm 0.6)$cm, that is very close to values obtained at more low energies.

In order to compare the nuclear production with that in proton-nucleon (pN) collisions we selected and measured additionally (along the larger length of primary track) 1064 inelastic events satisfying the criteria of interactions on the free and quasifree emulsion nucleons. The coherent interactions of protons on nuclei were separated from odd prong pN collisions following the criteria described in reference [2].

The tracks associated with each one of the interactions were classified , in accordance with the traditional emulsion terminology, into the following types:

a) black or b-particles with the range in emulsion $3\mu m < l < 3$mm, that corresponds to the kinetic energy of protons $T_p \lesssim 26$ MeV;

b) grey or g-particles having the range $l > 3$mm and ionization $I > 1.4 I_0$ (I_0 being the ionization due to the incident particle); this value of ionization corresponds to the velocity of singly-charged particle $\beta \lesssim 0.7$;

c) shower or s-particles having $I < 1.4 I_0$ ($\beta > 0.7$).

Multiplicity of these particles are designated as n_b, n_g and n_s, respectively. The black and grey particles together are referred to as heavily ionizing or heavy particles and $n_h = n_b + n_g$.

The emission angles of shower particles were measured carefully, so that, according to our estimate , the special method used for angular measurements gave an accuracy for

small angles not worse than $5 \cdot 10^{-4}$.

In the following we will consider three somewhat different samples of proton-nucleus interactions in emulsion.

1. The total ensemble of inelastic interactions produced by incident protons in emulsion, in all 3628 inelastic events.
2. Ensemble of interactions without coherent reactions and events due to the free emulsion hydrogen (the so-called "p-free-p" events) This sample of events consists of 3353 incoherent interactions corresponding to collisions with C, N, O ($\sim$27%) and Ag, Br ($\sim$73%) nuclei and hereafter will be referred to as pA interactions.
3. Ensemble of incoherent events (pEm collisions, in all 3482 events), i.e. the first sample purified from the coherent production.

As a rule, we will be analyzing in this paper the second sample of incoherent pA collisions containing exactly the same reactions as our π^-A and pA interactions at lower energies ($E_0 \lesssim$ 200 GeV), which are used here for comparison purposes. In all cases, when we shall consider the ensemble of pEm interactions with inclusion of coherent or p-free-p events (for the sake of comparison with data of other authors), this will be specially noted.

In conclusion of the Section, we would like to note that the coherent production by 400 GeV protons on emul-

sion nuclei is discussed in details in our paper [2], and the statistical separation of p-free-p interactions from pEm collisions has been performed in accordance with the method used in our previous works on hA interactions at lower energies (see, e.g. [3]).

3. Multiplicity of charged secondaries

3.1. Heavily ionizing particles

Figure 1 shows multiplicity distributions of black, grey and heavy particles for all considered ensembles of proton-nucleus interactions at 400 GeV and Table 1 presents the average multiplicities $\langle n_b \rangle$, $\langle n_g \rangle$, $\langle n_h \rangle$ and the ratio $\langle n_b \rangle / \langle n_g \rangle$ in comparison with those in pA and π^-A interactions at 200 GeV [3-5] .

The remarkable stability of the mean value $\langle n_h \rangle$ and n_h distributions in a wide energy range was observed and discussed in many experimental papers published earlier on hA interactions. Besides, in reference [4] it has been pointed out, as a result of an analysis of large statistical material on pA collisions in the range 7 - 200 GeV, that, although the multiplicity of h-particles does not change with energy, $\langle n_g \rangle$ slowly decreases with E_0 (from $\langle n_g \rangle$ = 3.6 at 7 GeV to $\langle n_g \rangle$ = 2.7 at 200 GeV). Our data (Table 1) demonstrate, in agreement with the recent results of other experiments at 200, 300 and 400 GeV [6], that the average multiplicity of all types of heavi-

ly ionizing particles in pA collisions is independent of energy at $E_0 \geqslant 200$ GeV. Taking into account the data of reference [4], one can extend this statement to the region of $E_0 \geqslant 50$ GeV. It is interesting to note, by the way, that just in this region of incident energies a number of approximate scaling regularities were observed for multiplicity of particles produced in hadronic collisions (see, e.g. reviews [7,8]).

The other interesting conclusion, following from the data of Table 1, is that the mean multiplicities of g and b-particles (and of h-particles as well) in high-energy $\pi^- A$ collisions are lower than in pA interactions. This circumstance is explained well by model approaches (of eikonal type, for instance), in which the difference between inelastic pion-nucleon and proton-nucleon cross sections is taken directly into account. One can note also that an amount of "large stars" (i.e. events belonging to the so-called total aplitting of heavy target nucleus with $n_h \geqslant 28$) is different in pA and $\pi^- A$ collisions and at 200 GeV equals $(2.6 \pm 0.2)\%$ and $(1.2 \pm 0.2)\%$, respectively.

The limiting behaviour of multiplicities of nuclear fragmentation products in interactions of elementary particles with nuclei contradicts the cascade-evaporation

model *) and is consistent with modern approaches to the theory of nuclear production, which are based on the consideration of space-time evolution in multiple production [7,8].

3.2 Shower particles

In Figure 2a we have plotted n_s distributions for all considered samples of interactions at 400 GeV and in Figure 2b that for the pA ensemble in the scaling variables. Table 2 gives the average value of shower particle multiplicity and the ratio $R = \langle n_s \rangle_{pA} / \langle n_{ch} \rangle_{pp}$, where for the latter we used $\langle n_{ch} \rangle_{pp} = 8.99 \pm 0.11$ obtained in pp interactions at 405 GeV [10]. Figure 3 shows the energy dependence of $\langle n_s \rangle$ and R in hEm interactions at high energies; for comparison the data on $\langle n_{ch} \rangle$ in hp collisions are plotted too (the data compiled in the review [8] were taken for these plots).

We can conclude from these data:

1. In the energy range considered ($E_0 \leq 400$ GeV), multiplicity of shower particles in hEm interactions increases with primary energy steeper than $\langle n_{ch} \rangle$. The normalyzed multiplicity R increases too, though at $E_0 > 200$ GeV a rate of growth decreases noticeably, being consis-

*) In fact, one can infer from reference 9 that the cascade-evaporation model with many-body interactions predicts for pA collisions at 400 GeV that $\langle n_b \rangle \simeq 9.2$, $\langle n_g \rangle \simeq 3.7$, and $\langle n_h \rangle \simeq 12.9$.

tent with many models of hA interactions, predicting the asymptotic independence of R on E_o. Moreover, if one takes into account that $\langle n_{ch} \rangle$ contains recoil protons, whereas a considerable amount of them is not included in $\langle n_s \rangle$, then, as well known from several papers, R becomes a constant at much low energies ($E_o \sim 50$ GeV, see, e.g. [3 - 5]).

2. n_s distribution at 400 GeV can be satisfactorily described by the same KNO scaling function, which has been determined by fitting experimental data on pA interactions in emulsion at $E_o > 50$ GeV [3] (see Figure 2b).

3. We have performed at our energy a calculation of n_s distribution according to a simple version of two-stage model (see, for details [3]), particular realizations of which correspond to the energy-flux cascade model (EFC) [12] and the two-phase model of hadronic matter (TPM) [11]. Also, we compared n_s distribution with predictions of the eikonal model developed by Shabelsky [13] . It is seen from Figure 2a, that Gottfried's model is explicitly ruled out by the data, whereas for models [11, 13] one can state more or less satisfactory agreement.

4. Comparing the energy dependences of $\langle n_s \rangle$ and R in πEm and pEm collisions one can conclude that shower particle multiplicity in the former is considerable lower. Again , this circumstance has a simple explanation in the framework of eikonal type models, in which the intranuclear col-

lisions of an incident particle and/or fast "cluster" play the decisive role in particle multiplication.

In order to determine the A dependence of $\langle n_s \rangle$, one can parametrize $\langle n_s \rangle = \langle N_{ch} \rangle A^{\alpha}$ and by using the expression

$$R = \sum_i N_i \sigma_i A_i^{\alpha} / \sum_i N_i \sigma_i \quad , \qquad (1)$$

N_i being a density of i-th type nuclei in emulsion , σ_i being the corresponding cross section, one gets that the experimental value of $R = 1.86 \pm 0.03$ leads to the result that $\alpha = 0.15 \pm 0.01$. This value of α coincides within experimental errors with that obtained recently for interactions of 400 GeV protons on pure metals [34]. So, we conclude, this dependence is weak just as at more low energies. Indeed, it has been claimed earlier [3-5] that such value of α is consistent with practically all the theoretical predictions, except for that of the naive cascade-evaporation model.

Let us now consider the behaviour of the normalysed and the central moments of shower particle multiplicity distribution with the incident energy, which is well known for n_{ch} distribution in hp collisions. Figure 4 presents the k-th roots of the central moments $\sqrt[k]{\mu_k} = \sqrt[k]{\langle (n_s - \langle n_s \rangle)^k \rangle}$ and the values of the normalyzed moments $C_k = \langle n_s^k \rangle / \langle n_s \rangle^k$ (for k=1-4) as functions of $\langle n_s \rangle$ and E_o, respectively . For comparison the straight lines representing the same quantities in pp interactions are plot -

tea. It is seen from these plots that there is at least the qualitative similarity between pA and pp collisions. This may be considered as an indication to the similarity of the production mechanisms in both interaction classes and obviously should be explained by any model pretending to describe the nuclear production.

3.3 Multiplicity correlations

In Figure 5 correlation dependences between multiplicities of different particles of the type $\langle n_i\ (n_j)\rangle$ ($n_i, n_j = n_s, n_b, n_g, n_h$; $i \neq j$) are shown for pA interactions at 400 GeV. It is seen that like the data at more low energies [3-5] such correlations may be fitted satisfactorily by linear functions with positive slopes

$$\langle n_i\ (n_j)\rangle = a_{ij} \cdot n_j + b_{ij}\ , \qquad a_{ij} > 0\ . \qquad (2)$$

Table 3 presents the values of coefficients a_{ij}, b_{ij} obtained by fitting experimental data; it should be noted that for n_g dependences the fit has been done only up to $n_g = 9$, since they show there a change in the slope (the so-called "saturation" effect).

Comparing the data of Table 3 and Figure 5 with those at energies $\leq$ 200 GeV [3-5], we can see that coefficients a_{sj} and b_{sj} remain to be growing with incident energy. This is easy to understand remembering that $\langle n_s\rangle$ increases for heavy particle multiplicities, which are already independent of E_o. However, it should be mentioned, that

b_{sj} is larger noticeably than $\langle n_{ch}\rangle_{pp}$ and the difference $b_{sj} - \langle n_{ch}\rangle_{pp}$ grows with E_o [4]. This means, in particular, the criterium used in emulsion cosmic ray experiments to select hadron-nucleon interactions in accordance with smallness of n_h is not satisfactory in the range of very high energies.

The data obtained do not contradict the important assumption that there is the positive correlation between the average number of target fragments and the so-called mean number of intranuclear collisions $\langle \nu \rangle$. However, it was shown [4,5], that due to different A dependence of these quantities ($\langle n_g\rangle$, $\langle n_b\rangle$, $\langle n_h\rangle \sim A^{2/3}$ and $\langle \nu \rangle \sim A^{1/3}$) in a wide energy range, the relation between them should be non-linear. Since the dependence $\langle n_s\ (n_g)\rangle$ is the strongest among $\langle n_s\ (n_j)\rangle$, we can assume that the best experimental measure of the number of intranuclear collisions, $\langle \nu \rangle$, is given by n_g, the number of grey particles.

4. Angular distributions of shower particles

Angular spectra of particles produced are still one of the basic sources of information about one-particle distributions in high-energy hA interactions. We will be using here as angular variable the pseudorapidity $\eta = -\ln\ \mathrm{tg}\ (\theta/2)$, where θ is the polar angle of a shower particle in the laboratory frame. As is well known, it gives for relativistic pions a good approximation of the

longitudinal rapidity $y = (1/2)\,\ln[(E+p_\ell)/(E-p_\ell)]$

According to many theoretical approaches, the parameter determining a hA collision is the value of ν, which, in the framework of models with repeated intranuclear collisions (where an interaction could be considered as some superposition of intranuclear collisions with separate nucleons) has the meaning of the effective number of encounters inside the nucleus or of the thickness of nuclear matter interacting with the incident particle in the framework of models where the target should be considered as structureless medium. It is common belief, justified by many experimental findings (see , e.g. [9]), that the number of nuclear fragments, especially those having momenta far from the evaporation region, is a good measure of ν ; indeed, it has been pointed out in several papers that it is reasonable to use the number of grey particles composed mostly of recoil protons for this purpose. Below we are using n_g as the main parameter characterizing a nuclear interaction in the sence considered. However, we have directly tested that all our qualitative conclusions concerning n_g dependence of the characteristics studied also remain true for n_h dependence.

Figure 6 shows inclusive η distributions for pA and pN collisions at 400 GeV in comparison with those for pA interactions at 50 and 200 GeV [16] and for π^-A interactions at 200 GeV [5]. Figure 7 presents η plots for the

n_g groups of pA interactions in comparison with some selected data at more low energies [16] .

One can conclude from these data, that:

1. η distributions in hA interactions become wider with increasing E_0, but part of the distributions at $\eta \lesssim 1$ (target fragmentation region) remains unchanged. This is the phenomenon of limiting fragmentation, that is well-known from elementary collisions. However, it should be noted, that the limiting behaviour is also characteristic of events with any fised n_g. i.e. of events corresponding to the fixed impact parameters in terms of geometrical models.
2. There is an indication, although rather weak, to the appearence of bimodality in inclusive η distributions in pA collisions at 400 GeV (see Figure 6). This is of interest in connection with the bimodal structure, which has been recently observed with confidence in π^-A interactions at 200 GeV [5] . If the existence of such a structure will be confirmed by further experiments (as well as the fact that it appears at more low energies for pion induced reactions), this might be considered, in our opinion, as the strong support to the models of repeated intranuclear collisions (see also the discussion of this topic in [16]).
3. When n_g increases η distributions undergo deformation in such a way that contribution of shower particles

with low η increases too. Although in pA interactions at 400 GeV they do not demonstrate the bimodality so evi - dently, as in π^-A interactions at 200 GeV, one can ob - serve a shoulder at large n_g (see Figure 7) corresponding to the position of the maximum of η distribution ($\eta \simeq 4$) in pN interactions at the same incident energy.

For the detail analysis of E_0 and A dependences of angular spectra we have considered the differences

$$d = \frac{1}{\sigma_{pA}} \frac{d\sigma}{d\eta} pA - \frac{1}{\sigma_{pN}} \frac{d\sigma}{d\eta} pN \qquad (3)$$

and the ratios

$$r = \frac{1}{\sigma_{pA}} \frac{d\sigma}{d\eta} pA \Big/ \frac{1}{\sigma_{pN}} \frac{d\sigma}{d\eta} pN \qquad (4)$$

for the n_g groups of pA interactions, where the following normalization is used $\int \frac{1}{\sigma} \frac{d\sigma}{d\eta} d\eta = \langle n_g \rangle$ for the corresponding subensemble. Figure 8 shows d and r as functions of η for the total ensemble of pA inter- actions and Figures 9 and 10 the same quantities for su- divisions with different n_g. For comparison in Figures 8a and 9 the data are plotted at more low energies and the curves in Figure 8b correspond to two versions of the parton-cascade model: the curve 1 represents predic- tions of the model which is based on the so-called fan type diagrams only [17] and the curve 2 belongs to the model including additionally two-ladder exchanges [18].

It is seen from the data th t the value of pseudorapidity ($\eta_0 \simeq 6.0$ for pA interactions at 400 GeV) giving the equality

$$\frac{1}{\sigma_{pA}} \frac{d\sigma}{d\eta} pA = \frac{1}{\sigma_{pN}} \frac{d\sigma}{d\eta} pN$$

within errors is independent of the number of slow par - ticles (i.e. A*) and increases with primary energy. This is inconsistent with the particular version of the multi- peripheral model (MPM) of hA interactions [19], which predicts that the value of longitudinal rapidity y_0^* cor- responding to η_0 in the c.m. frame ($y_0^* \simeq \eta_0 - \mathrm{Arch}\, \gamma_c$, γ_c being the Lorentz factor of the c.m. frame in the labora- tory one) should depend on A, being independent of E_0 at high energies.

The shape of the difference d changes and its center shifts towards low η with n_g (see Figures 8a,9). The sa- me was observed earlier for nuclear production at $E_0 \lesssim$ 200 GeV [5,16,20] and this is completely inconsistent with the energy-flux cascade model [12]. The width of d increases with E_0 like the width of η distribution (compare with Figure 6).

---

*) As can be seen from the recent electronic experiment performed at the FNAL [33], this is also true for neut- ron-nucleus collisions at high energies.

At $\eta > \eta_0$, the ratio r decreases with n_g in such a way that the larger the η, the smaller r becomes (Figure 10). This is the so-called "extinction" of leading particles, known from experiments at lower energies (see, e.g. the review [8]). As is seen from Figure 8a and the comparison of the data on r at different E_0 (not shown here), this effect does not weaken at least up to 400 GeV.

At $\eta < \eta_0$, r increases with n_g (and $\langle \nu \rangle$), so that the smaller the η, the larger r becomes. It is important that the A dependence of the ratio r changes with η monotonically, without any singularities, expected, for instance, in the framework of the EFC [12], MPM [19] and some other models of nuclear production. Assuming that shower particle multiplicity in different η intervals may be parametrized as $\Delta n_g(\eta, E_0) \sim A^{\alpha(\eta, E_0)}$, one can observe that the exponent α monotonically increases from negative values at maximal η to values of about 0.4-0.5 at minimal η. Figure 11 examplifies such dependences: here it should be remembered that we qualitatively identify n_g and A dependences by using the relation $\langle n_g \rangle \sim A^{2/3}$.

One can conclude from the direct comparison of the data with quantitative predictions of the parton-cascade model (PCM) [17,18] that it cannot describe the η dependence of the ratio r. It is very important that, even

at 400 GeV, the data do not demonstrate the "limiting" behaviour ($r \to 1$) at large rapidities, which arises in these models due to the fastest noninteracting part of a parton ladder [21]. Also, it should be noted that inclusion of a small contribution of double scatterings does not inprove the situation considerably (compare curves 1 and 2 in Figure 8b).

The disagreement of experimental data with predictions of the PCM, which assumes the predominance of fan type diagrams [17,18,21] may be considered as an indication that probably the eikonal type models [22] are more preferable for description of nuclear production in the range of presently available energies and for actual nuclei; such an approach is close from the phenomenological viewpoint to the celebrated Glauber theory of multiple scattering. It should be noted that earlier the same conclusion has been drawn from the analysis of nuclear production data at $E_0 \leq 200$ GeV [16].

The most apparently the absence of the limiting behaviour discussed above follows from Figure 12, where the quantity $y_{max} - \eta_0$ ($Y_{max} = \ln(2E_0/m)$ is the kinematical limit of rapidity) is plotted versus the primary energy E_0. According to the PCM [17,18,21], the limiting behaviour of η distributions at largest rapidities leads to the increase of $Y_{max} - \eta_0$ with E_0 [18]. On the other hand, in the Glauber-Gribov model [22] this quantity

should be a constant equal to $\simeq 2.6$. The data give the strong support to the second approach, although, of course, it is necessary to check model in many points to give more confident and reliable conclusions about its applicability.

Let us now consider the A dependence of the centers and dispersions (more exactly standards) $\sigma(\eta)$ of shower particle angular distributions. From Figure 13, where these characteristics of η distributions are presented in dependence on n_g, we see that they decreases with increasing number of grey particles.

It has been shown in reference [16] that the A dependence of dispersions of inclusive η distributions provides us with a good test for models based on the assumption that : i) an incident hadron collides simultaneously with all the nucleons, containing in a tube of nuclear matter with a cross section equal to σ_{hN} and the mass much greater than the nucleon mass, and ii) such an interaction looks like a hadron-nucleon collision at some higher c.m. energy. In the framework of such models, the extreme realisation of which is presented by the coherent or collective tube model [23], the dispersion of "longitudinal" inclusive distributions must increase with increasing A; this is the straightforward consequence of the logarithmic growth of dispersions in elementary collisions (as is well-known $\sigma(y) \sim \ln s$).

As is seen from Figure 13, the dependence of $\sigma(\eta)$ on n_g contradicts that calculated according to the CTM. Obviously, the same is also true for related models, such as discussed in papers [24,25]. Of course, it should be noted that this conclusion cannot be extended to "tube" models in which a hadron-tube collision is taken to be different from hadron-nucleon interaction. For example, in the hydrodynamical model the final state of produced system is conditioned not only by larger c.m. energy, but by larger volume of the incident system as well; in other words, the final state is conditioned by the initial densities of thermodynamic quantities [26].

It is well known that the simple and attractive notions of collective interaction with a "tube" of nuclear matter and the passivity of fastest secondaries inside the nucleus are originated from the hypothesis that there exists some characteristic length $L \sim kE$ (E being the energy of a particle and $k \simeq 10^{-13}$ cm/GeV) which is necessary to "materialize" that particle. The data on hA interactions at $E_0 \lesssim 400$ GeV show that, even if this hypothesis is true, the region of its applicability should be shifted towards considerably higher energies.

Some indication to the energy range, where this hypothesis is probably true, follows, maybe, from Figure 14, where the energy dependence of $\sigma(\eta)$ is plotted for different n_g groups of pA interactions. One can see that

with increasing E_0 the difference between $\sigma(\eta)$ for different n_g groups decreases (especially for events with small n_g) and has a good chance to disappear at $E_0 \sim 10^{13}$ eV (if one uses the linear extrapolation). It is possible that only at such very high energies the collective phenomena in hA interactions will manifest themselves strongly. This suggestion, of course, needs the direct experimental test in hA interactions at $E_0 > 10^{12}$ eV, that is impossible to perform at present.

5. Two-particle correlations

5.1. Pseudorapidity correlations among shower particles

There are little data on correlations in hA interactions [5, 8,16,27-30], although they are very useful [8, 16,31] for discrimination between various (not infrequently conflicting in exiomatic approaches) models suggested for nuclear production.

In order to study two-particle correlations among shower particles along the longitudinal axis we have used the well-known correlation functions

$$C_2(\eta_1^*, \eta_2^*) = \frac{1}{\sigma_{in}} \frac{d^2\sigma}{d\eta_1^* d\eta_2^*} - \frac{1}{\sigma_{in}^2} \frac{d\sigma}{d\eta_1^*} \frac{d\sigma}{d\eta_2^*}, \quad (5)$$

$$R_2(\eta_1^*, \eta_2^*) = \sigma_{in} \frac{d^2\sigma}{d\eta_1^* d\eta_2^*} \Big/ \frac{d\sigma}{d\eta_1^*} \frac{d\sigma}{d\eta_2^*} - 1, \quad (6)$$

where η^* is the pseudorapidity in the proton-intranuclear nucleon c.m. frame

$$\eta^* = \eta - \mathrm{Arch}\, \gamma_c . \quad (7)$$

γ_c being the Lorentz factor of this frame in the laboratory one.

As has been emphasized in references [5,8,27], it the study of correlations by means of correlation functions (5,6) one is faced with the difficulties, which arise from taking quantitative account of pseudocorrelations arising from the broad multiplicity distributions of shower particles, the dependence of the one-particle spectrum ($d\sigma / d\eta$) on n_s and the possible realization of different production mechanisms, as well as trivial correlations due to kinematical coinstraints in individual events. While considering hA collisions, the obvious heterogencity of events corresponding to different number of intranuclear collisions or "tube" lengths strengthens these difficulties even in the case of the exclusive channel. Therefore, the precize model-independent search for dynamical correlations seems to be impossible in hA interactions [5].

The empirical information on correlation functions and their dependence on the atomic number of a target and on the incident energy is of great importance, although the reliable conclusions about the consistence of some model approach with nuclear production data could be obtained. strictly speaking, only by the direct confrontation of

experimental data with the values of C_2, R_2 calculated in the framework of that model, taking account of experimental conditions. However, one can hope, that even the qualitative comparison of the data with model expectations can give, in some cases, the useful information about applicability of some model approaches.

In close analogy with reference [5], we will consider the number of grey particles n_g as the main parameter determining qualitatively the A dependence of observables. We will be analyzing, together with the correlators C_2 and R_2, the "quasidynamical surpluses" $C_2' = C_2 - C_2^{IEM}$ and $R_2' = R_2 - R_2^{IEM}$, where C_2^{IEM} and R_2^{IEM} are the correlators calculated by the Monte Carlo method in accordance with the simple independent emission model (IEM). We assumed in this model, that:

i) the n_s distribution in each ensemble of Monte Carlo events reproduces the empirical n_s spectrum of the real ensemble;

ii) the one-particle spectrum $d\sigma / d\eta$ in each one of the simulated interactions reproduces the empirical semi-inclusive distributions $d\sigma/\eta\, d\eta$ in collisions with the corresponding n_s for the ensemble under cosideration;

iii) the emission angles of shower particles are independent statistically.

As has been shown in reference [30], conservation laws in the form inherent to the statistical theory of

multiple production weakly diminish C_2 and R_2 compared with C_2^{IEM}, R_2^{IEM} at $\Delta\eta = |\eta_1 - \eta_2| \lesssim 2$ in the range of tens and hundreds GeV. Therefore, the omission of conservation laws in the IEM only increases the dynamical significance of the inequalities $C_2' > 0$, $R_2' > 0$ at small $\Delta\eta$. For the reader, who, maybe, will be astonished by application of such crude model as the IEM for the analysis of correlations in hA collisions, we can only remind that in nuclear interactions the precize account of kinematical correlations is impossible due to the impossiblity of determination of the real mass of the target and separation of secondaries into those "produced" during the production process and those emitted by the nucleus after the encounter - in any case one needs some model (i.e. speculative) assumptions.

Let us now consider the experimental data. Figure 15 presents values of the correlators C_2, R_2 for arguments (η_1^*, $\eta_2^* \simeq \eta_1^*$) (the diagonal of correlation matrix, characterizing the magnitude of "short-range" correlations at different η^*) and (0, η^*) in pA and pN interactions at 400 GeV. The corresponding values of C_2' and R_2' are plotted in Figure 16. Figure 17 and 18 show the energy dependence of the correlators C_2, R_2 and C_2', R_2', respectively in pA collisions (the data at 24, 67 and 200 GeV are taken from reference [30]). The analysis of these data results in the following conclusions:

1. The values of the correlators in pA interactions differ significantly from those in pN collisions. The difference is large especially in the target fragmentation region. It is clear, nevertheless, that the strong asymmetry of correlation functions in pA interactions has mainly the trivial origin, in contrast with the conclusion of [29] by the way, since it is described by the IEM. This asymmetry can be explained by pseudocorrelations caused by large values and fluctuations of multiplicity and one-particle distributions in the target fragmentation region.

2. The correlator C_2 strongly depends on E_o, whereas R_2 demonstrathe the remarkable, though approximate, stability to the variation of energy in the range 20-400 GeV. These features of R_2 and C_2 are quite similar to those observed for two-particle correlations in hN interactions (see, e.g. [32]).

3. Values of the "quasidynamical surpluses" C_2' and R_2' for small $\Delta\eta^*$ in pA interactions are positive everywhere, except the region of the largest η^* -the region of the leading particles. The function C_2' increases with increasing E_o; for the R_2' one can observe the approximate independence on E_o. Thus, the data exhibit the presence of positive short-range correlations in pA interactions (as well as in pN collisions), which cannot be explained by the simplest trivial and kinematic factors. Of course, we

FERMILAB-PUB-78-135-E

have noted above, that the values $\hat{C}_2'$, $R_2' > 0$ can also be caused by the heterogeneity of one-particle spectra for individual collisions with fixed n_s, i.e. by the reason that is very trivial for nuclear production. Some qualitative considerations concerning the comparative significance of genuine dynamical correlations and those caused by the angular heterogeneity will be presented below.

4. Comparing the correlators R_2, R_2' for pA interactions in the range 20-400 GeV with those in $\pi^- A$ collisions at 200 GeV [5], one can conclude that correlations among relativistic secondaries weakly depend on the nature of the projectile.

Now we consider the dependence of correlation functions in pA interactions at 400 GeV on the number of grey particles assuming the existence of positive correlations between $\langle n_g \rangle$ and $\langle \nu \rangle$. Figure 19 presents values of the correlator $R_2(\eta_1^*, \eta_2^* \approx \eta_1^*)$, $R_2(0, \eta^*)$ and Figure 20 shows $R_2'(\eta_1^*, \eta_2^* \approx \eta_1^*)$ for some selected subensembles of pA collisions with different n_g. One can conclude from these data, that:

(i) shapes of the correlators R_2 and R_2' in subensembles with different n_g qualitatively are similar and differ from those in pN collisions;

(ii) the values of R_2 and R_2' decrease with increasing n_g at all pseudorapidities except the region of leading particles. Here we took into account that the action of con-

servation laws becomes less with n_g at least due to positive correlation between $\langle n_s \rangle$ and $\langle n_g \rangle$, so that the degree of understating of R_2^1 at $\Delta\eta^* \lesssim 2$ caused by employing the IEM increases with decreasing n_g.

Although the quantitative model calculations are absent for the correlators in hA interactions, the data obtained allow one, in our opinion, to draw some qualitative conclusions.

The A dependence of the inclusive correlators in high-energy hA interactions seems to be hardly consistent with the CTM and the related models [22-25], in which a hadron-tube collision is identical entirely with a hadron-nucleon interaction at more high c.m. energy s. In fact, since according to the CTM, the inclusive density of rapidity distribution in hA interactions is given by the sum of inclusive hN densities

$$\rho_{hA}(y,s) = \sum_{\nu} P(\nu)\, \rho_{hN}(y + \tfrac{1}{2}\ln\nu, \nu s), \quad (8)$$

the difference between whose centers at high energies is much less than their dispersions, and since R_2 in hN interactions does not depend on s [32], one should expect that in nuclear production the correlator R_2 would depend very weakly (if at all) on the atomic number of a target. In order to prove this statement quantitatively we have calculated in accordance with the CTM the values of R_2 by the Monte Carlo method for different nuclei and for the

composite target such as emulsion. In this calculation the Woods-Saxon distribution was taken for nuclear densities and we used the Gaussian for pseudorapidity distributions in hN collisions. The results of a calculation, which are represented in part in Figure 19 by the curves, in fact were found to be practically independent of A. So we conclude, the data of Figure 19 contradict the predictions of the CTM. This conclusion, strictly speaking, cannot be extended to tube models where hadron-tube and hN interactions are not taken to be similar.

The decrease of R_2 with increasing number of recoil protons agrees well, although qualitatively, with predictions of the PCM, which takes into account the limited energies of particles participating in intranuclear collisions [31].

Also, it has been claimed in [31], that the inequality $R_2^{hA} < R_2^{hN}$ in eikonal type models, where only the leading particle (or leading cluster) undergoes intranuclear collisions, will be realized only in the projectile fragmentation region. The data show that this inequality is realized in larger part of the central region as well. Remembering that the prediction has purely the qualitative character and due to uncertainties in definition of fragmentation and central regions at our energy, we think that this model in that point does not disagree enough with the data to be ruled out.

The comparison of the functions R_2' in the total sample of pA interactions and in different n_g groups (Figure 20) demonstrates, to our mind, the significant role of heterogeneity of nuclear events in the formation of "short-range" correlations. In fact, if the idea about the relation between $\langle n_g \rangle$ and $\langle \nu \rangle$ is correct, then the full ensemble of pA events should be, especially in the target fragmentation region, more heterogeneous than comparatively narrow n_g groups. Consequently, the correlators should be larger for the total ensemble of pA interactions. Just this is observed in the data.

On the other hand, the decrease of R_2 and R_2' with increasing n_g at small $\Delta\eta^*$ may be considered as indication of genuine dynamical correlations, since the heterogeneity of interactions probably does not decreases with increasing n_g [5]. In any case, it seems to us, that for more confident and reliable conclusions about the nature of such dynamical correlations it is necessary to have more accurate data with pure targets as well as more suitable methods for analysis of correlations.

5.2. Azimuthal correlations

The study of correalations in the transverse plane (azimuthal correlations) is of great importance since they can clarify the production mechanism in high-energy interactions. For example, the large transverse momentum

of decaying system may lead to the asymmetrical emission of particles in the transverse plane; the large transverse momenta of two clusters (Jets) or large angular momentum transfer may result in the coplanar emission and so on.

We studied two-particle inclusive and semi-inclusive azimuthal correlations among particles produced in pA and pN interactions employing the asymmetry and coplanarity coefficients

$$A = \left(\int_{\pi/2}^{\pi} \rho(\varepsilon)\,d\varepsilon - \int_{0}^{\pi/2} \rho(\varepsilon)\,d\varepsilon\right) \Big/ \int_{0}^{\pi} \rho(\varepsilon)\,d\varepsilon, \quad (9)$$

$$B = \left(\int_{0}^{\pi/4} \rho(\varepsilon)\,d\varepsilon + \int_{3\pi/4}^{\pi} \rho(\varepsilon)\,d\varepsilon - \int_{\pi/4}^{3\pi/4} \rho(\varepsilon)\,d\varepsilon\right) \Big/ \int_{0}^{\pi} \rho(\varepsilon)\,d\varepsilon, \quad (10)$$

where

$$\rho(\varepsilon) = d\sigma/d\varepsilon, \; \varepsilon \equiv \varepsilon_{12} = \arccos(p_{t1} p_{t2} / |p_{t1} p_{t2}|). \quad (11)$$

In order to take into account trivial effects related to the action of conservation laws we have performed calculations for pA and pN interactions on the basis of the cylindrical phase-space model (CPS) under the following assumptions:

1. the n_s distribution in each ensemble of simulated events reproduces the empirical n_s spectrum of the real ensemble in pA and pN interactions;
2. the multiplicity of neutral pions at fixed n_s obeys the truncated binomial law with the mean value obtained at 405 GeV from the FNAL bubble chamber experiment;

3. the presence of "non-observable" (i.e.not incoming n_s) recoil nucleons in pA interactions has been taken into account by means of the simple model of repeated intranuclear collisions described in [2] under the assumption that nuclear densities obey the Woods-Saxon distribution.

Figures 21 a,b present, as examples, the values of the asymmetry and coplanarity coefficients A,B in semi-inclusive pA and pN interactions for not very large n_s in comparison with calculated dependences. It is seen that the data agree quite satisfactorily with the calculations. Consequently, the data do not demonstrate any anomalies which cannot be described by the simple statistical considerations. The same was concluded for hA interactions at lower energies [4,5,8,27] .

Also, we have considered the dependence of A and B on the relative distance $\Delta\eta$ along the pseudorapidity scale for two particles considered (not shown here). Similarly to π^- A interactions at 200 GeV [5] , we could not observe any dependence of these quantities on $\Delta\eta$, that means the correlations among secondaries in the azimuthal plane have mainly the long-range nature.

6. Concluding remarks

Let us now summarize the results drawn from investigation of inelastic pA interactions at 400 GeV and from consideration of the energy and atomic number dependences of some basic characteristics of hA interactions at presently available energies.

The detailed comparison of esperimental data with qualitative and quantitative predictions of various theoretical approaches to multiple production on nuclei shows apparently that most of them cannot describe the complete set of existing data. First of all, we should attribute to them the following models: the naive cascade-evaporation model, the energy-flux cascade model, the coherent tube and related models, some well-developed in the quantitative respect versions of the multiperipheral and/or parton model, models which do not include any cascading except the repeated collisions of the leading particle .

The eikonal models based upon the Glauber-Gribov theory and the hydrodynamical model have, to our mind, the best chances to survive. However, the question about the consistence of two these rather general approaches with the data should be considered as undecided since presently we have only some semi-quantitative model predictions and any conclusion about their applicability may be considered as proven only after the detailed quantitative comparison of their predictions with the data.

The complete set of experimental data available allow us to assume that the production mechanism in hA interactions has probably two- or multi-component character and contributions of separate components may depend on the

energy and the atomic number of a target [8] .

Finally, we claim that the present status in the study of inelastic hadron-nucleus collisions does not exclude the possibility to obtain the fundamental information about the nature of strong interactions (in particular, about the space-time evolution of multiple production and the internal structure of hadrons) and therefore, we believe, this field remains to be interesting and fashionable.

Acknowledgements

We wish to thank the managements of the FNAL and the Division of Nuclear Physics of the Academy of Sciences of the USSR for the support of the experiment and L.Voyvodich and I.V.Chuvilo for the help during exposition. We are ver indebted to A.I.Bondarenko and V.Sh.Navotny for the invaluable help during the data processing and computing. Finally, the work carried out by technical staffs of our laboratories is gratefully acknowledged.

Рукопись поступила в
Издательский совет
24 мая 1978г.

R E F E R E N C E S

1. Alma-Ata-Gatchina-Moscow-Tashkent collaboration, Lebedev Inst. preprint 43, Moscow, 1977; ZhETF Pis'ma 25 (1977) 309.
2. Alma-Ata-Gatchina-Moscow-Tashkent collaboration, Lebedev Inst. preprint 61, Moscow , 1977.
3. Alma-Ata-Leningrad-Moscow-Tashkent collaboration, Yadernaya Fizika 22 (1975) 736.
4. A z i m o v S.A. et al., Proc.of the Topical Meeting on multiparticle production on nuclei at very high energies, Trieste, 1976, ed B e l l i n i G. et al., p.83; Yadernaya Fizika 26 (1977) 346.
5. Alma-Ata-Gatchina-Moscow-Tashkent collaboration, Nucl. Phys. B129 (1977) 205.
6. O t t e r l u n d I. et al., Lund Univ.preprint LUTP-7705, Lund, 1977.
7. N i k i t i n Yu.P., R o z e n t a l I.L. and S e r g e e v F.M., Uspekhi Fizicheskhikh Nauk 121 (1977) 3.
8. G u l a m o v K.G., G u l y a m o v U.G. and C h e r n o v G.M., Particles and Nuclei 9 (1978) No 3.
9. B a r a s h e n k o v V.S., T o n e e v V.D., Interactions of high energy particles and nuclei with nuclei (Atomizdat, Moscow) 1972.
10. B r o m b e r g C. et al., Phys.Rev.Lett., 31, (1973) 1563.

11. F i s h b a n e P.M. and T r e f i l J.S., Phys.Lett. B51 (1974) 139.

12. G o t t f r i e d K., Preprint TH-1735 CERN,1973; Phys. Rev.Lett. 32 (1974) 957.

13. S h a b e l s k y Yu.M., Konstantinov Inst.preprint LNPI-248,Leningrad, 1976; Yadernaya Fizika 27 (1977) 1084.

14. M o l l e r K., Nucl.Phys. B79 (1974) 1451.

15. W r o b l e w s k i A., Acta Phys.Pol. B4 (1973) 857.

16. A z i m o v S.A. et al., Yadernaya Fizika,27,1011,1978.

17. N i k o l a e v N.N., Landau Inst.Preprint 18, Chernogolovka, 1975; Proc.of the Topical Meeting on multi - particle production on nuclei at very high energies, Trieste 1976, ed. B e l l i n i G. et al.

18. N i k o l a e v N.N. and O s t a p c h u k A.V., Nucl. Phys. B, 134, 729, 1978.

19. K o p l i k J. and M u e l l e r A.H., Phys.Rev. D12 (1975) 3638.

20. A n d e r s s o n B. and O t t e r l u n d I., Nucl. Phys. B102 (1976) 238.

21. K a n c h e l i O.V., ZhETF Pis'ma 18 (1973) 469.

22. C a p e l l a A. and K a i d a l o v A., Nucl.Phys. B111 (1976) 477.

23. B e r i a d G. et al., Phys.Rev.D13 (1976) 161; A f e k Y. et al., Proc. of the Topical Meeting on

FERMILAB-PUB-78-135-E

multiparticle production on nuclei at very high energies, Trieste 1976, ed. B e l l i n i G. et al.

24. M e n g T a - c h u n g , Phys.Rev.D15 (1977) 1977.

25. F r e d r i k s s o n S.Stockholm preprint TRITA-TFY-75-13, 1975; B e r g s t r o m L. and F r e d r i k s s o n S.,Phys.Lett.68B (1977) 177.

26. S h u r y a k E.V., Yadernaya Fizika 24 (1976) 630.

27. G u l a m o v K.G., C h e r n o v G.M. and Y u l d a s h e v B.S., Proc.of the 4 th Intern Seminar on the Problems of High Energy Physics, Dubna, 1975, p.233; A z i m o v S.A. et al., Multiple processes at High Energies (Fan. Tashkent, 1976) p.120.

28. Alma-Ata-Dubna-Leningrad-Moscow-Tashkent collaboration, ZhETF Pis'ma 24 (1976) 107.

29. B a r o n i G. et al., Nucl.Phys. B103 (1976) 213; Lett.Nuov.Cim. 18 (1977) 352.

30. G u l a m o v K.G. et al., Z.Phys. A280 (1977) 107.

31. N i k o l a e v N.N., ZhETF Pis'ma 24 (1976) 383.

32. K o W., Univ.of California preprint UCD-PPL-7-17-74, Davis 1974.

33. F e r b e l T. Univ. of Rochester preprint UR-625, Rochester 1977.

34. F u m u r e F. et al., Proc.of the 15 th Intern.Cosmic Ray Conf., Plovdiv 1977, v.7, p.59.

Table 1.

The mean multiplicities of heavily ionizing particles in hadron-nucleus interactions at 400 and 200 GeV

Ensemble of events	E_0, GeV	$\langle n_b \rangle$	$\langle n_g \rangle$	$\langle n_h \rangle$	$\langle n_b \rangle / \langle n_g \rangle$	Reference
pA collisions (3353 events)	400	5.00 ± 0.09	2.99 ± 0.06	7.99 ± 0.14	1.67 ± 0.06	this experiment
pEm collisions (3482 events)	400	4.76 ± 0.09	2.89 ± 0.06	7.65 ± 0.14	1.65 ± 0.06	- " -
All inelastic proton-nucleus interactions (3628 events)	400	4.62 ± 0.08	2.79 ± 0.06	7.41 ± 0.13	1.66 ± 0.06	- " -
pA collisions (2743 events)	200	5.0 ± 0.1	2.70 ± 0.06	7.7 ± 0.1	1.86 ± 0.06	[6]
π^-A collisions (4853 events)	200	4.52 ± 0.07	2.38 ± 0.04	6.89 ± 0.11	1.89 ± 0.05	[5]

Table 2.

Multiplicity of shower particles in proton-nucleus interactions at 400 GeV.

Ensemble of events	$\langle n_s \rangle$ *)	R
pA collisions (3353 events)	16.74 ± 0.17	1.86 ± 0.03
pEm collisions (3482 events)	16.42 ± 0.17	1.83 ± 0.03
All inelastic collisions in an emulsion (3628 events)	15.92 ± 0.17	1.77 ± 0.03

*) Without corrections due to the Dalitz pairs the mean number of which is equal $\approx 0.01 \langle n_s \rangle$.

FERMILAB-PUB-78-135-E

Table 3.

Results of the approximation to experimental data on multiplicity correlations by the dependence $\langle n_i (n_j) \rangle = a_{ij} n_j + b_{ij}$

$\langle n_i \rangle$ \ n_j	n_h	n_b	n_g *)	n_s
$\langle n_h \rangle$	-	$1.50\ n_b + 0.47$	$2.32\ n_g + 1.42$	$0.45\ n_s + 0.40$
$\langle n_b \rangle$	$0.63\ n_h + 0.00$	-	$1.32\ n_g + 1.42$	$0.27\ n_s + 0.47$
$\langle n_g \rangle$	$0.37\ n_h + 0.00$	$0.50\ n_b + 0.47$	-	$0.17\ n_s + 0.10$
$\langle n_s \rangle$	$0.76\ n_h + 10.49$	$1.09\ n_b + 11.54$	$2.03\ n_g + 11.20$	-

*) For n_g dependences, the fit has been done only up to $n_g = 9$

FIGURE CAPTIONS

Figure 1. Multiplicity distributions of black (a), grey (b) and heavy (c) particles in proton-emulsion nuclei interactions at 400 GeV. Singly and doubly shaded areas show contributions of "p-free-p" and coherent events, respectively.

Figure 2. Shower particle multiplicity distribution plotted in usual (a) and scaling (b) variables. Shaded and dotted areas show contributions of "p-free-p" and coherent events, respectively. The curves 1,2,3 represent predictions of the EFC [12], TPM [11] and Shabelsky's [13] models, respectively. The curve 4 is the KNO scaling function for pA interactions in emulsion [3]. Curves 1 and 2 belong to pA interactions and the curve 3 to the total ensemble of emulsion events.

Figure 3. $\langle n_s \rangle_{hEm}$, $\langle n_{ch} \rangle_{hp}$ (a) and R_{nEm} (b) as functions of the incident energy. The curves are hand-drawn fits to experimental data.

Figure 4. Dependences of D (a), $\sqrt[3]{\mu_3}$ and $\sqrt[4]{\mu_4}$ (b) on n_s and C_k on E_0 (c) for pA interactions. The data at $E_0 \leq 200$ GeV are taken from ref. 4. The solid lines are hand-drawn fits to pA interactions, the dashed lines represent results

of an approximation of experimental data on pp interactions [14,15] .

Figure 5. Multiplicity correlations in pA interactions at 400 GeV. The straight lines represent of an approximation with the function $\langle n_i \rangle = a_{ij} n_j + b_{ij}$.

Figure 6. Inclusive pseudorapidity distribution of s-particles in pA interactions at 400 GeV in comparison with those in pN (E_o = 400 GeV), pA (E_o =50, 200 GeV [4]) and $\pi^- A$ (E_o = 200 GeV [5]) interactions.

Figure 7. η plots for different n_g groups of pA (E_o =50 and 400 GeV) and $\pi^- A$ (E_o =200 GeV - the dotted histograms) interactions.

Figure 8. (a) the quantity d as function of η in pA interactions at 400 (the solid histogram - this experiment) and 50 GeV [16] (the dashed histogram); (b) the quantity r in dependence on η for pA interactions at 400 GeV. The curves represent predictions of the parton-cascade model [17,18] .

Figure 9. Dependence of the difference d on η for different n_g groups of pA interactions at 50 (dashed histograms taken from ref. [16]) and at 400 GeV.

Figure 10. The ratio r as function of η in different n_g groups of pA interactions at 400 GeV.

Figure 11. n_g dependence of the ratio $r(\eta)$: the data for $\eta \leq 0$, $0 < \eta < 1, \ldots, 6 < \eta < 7$ and $\eta > 7$ are plotted from the bottom.

Figure 12. The energy dependence of the quantity $Y_{max} - \eta_o$ (see text). The data at $E_o \leq 200$ GeV are taken from ref. [16.] The curves 1,2 belong to the parton-cascade model [17,18] .

Figure 13. n_g dependence of $\langle \eta \rangle$ (a) and $\sigma(\eta)$ (b) in pA interactions at 400 GeV.

Figure 14. The energy dependence of $\sigma(\eta)$ for the total ensemble of pA interactions and for different n_g groups. The data at $E_o \leq 200$ GeV are taken from ref. [16].

Figure 15. Inclusive correlators $C_2(\eta_1^*, \eta_2^* \approx \eta_1^*)$ (a) , $R_2(\eta_1^*, \eta_2^* \approx \eta_1^*)$ (b), $C_2(0, \eta^*)$ (c) and $R_2(0, \eta^*)$ (d) in pA (the black points) and pN (the open circles) interactions at 400 GeV. Predictions of the IEM (see text) are plotted: the solid curves - for pA interactions, the dashed curves - for pN interactions.

Figure 16. Inclusive correlators C_2' and R_2' for the examples shown in figure 15. The curves are hand-drawn fits to guide the eye.

Figure 17. The energy dependence of the correlators $C_2(\eta_1^*, \eta_2^* \approx \eta_1^*)$ (a), $R_2(\eta_1^*, \eta_2^* \approx \eta_1^*)$ (b), $C_2(0, \eta^*)$ (c) and $R_2(0, \eta^*)$ (d) in pA interactions .

The data at E_0 = 24,67 and 200 GeV are taken from ref. [4] . The curves belong to the IEM.

Figure 18. Inclusive correlators C_2' and R_2' for the examples shown in figure 17.

Figure 19. Dependence of the correlation functions $R_2(\eta_1^*, \eta_2^* \approx \eta_1^*)$ (a) and R_2 $(0, \eta^*)$ (b) on the number of grey particles in pA interactions at 400 GeV. The curves reproduce results of a calculation performed in accordance with the CTM (see text).

Figure 20. Correlators R_2' $(\eta_1^*, \eta_2^*, \approx \eta_1^*)$ in different n_g groups of pA interactions at 400 GeV.

Figure 21. Dependences of the azimuthal asymmetry coefficient A (a) and the complanarity coefficient B (b) on n_s in pN (the open circles) and pA (the black data points) interactions. The curves plotted are obtained according to the CPS model (see text) for pN (the curve 1) and pA (curve 2) collisions.

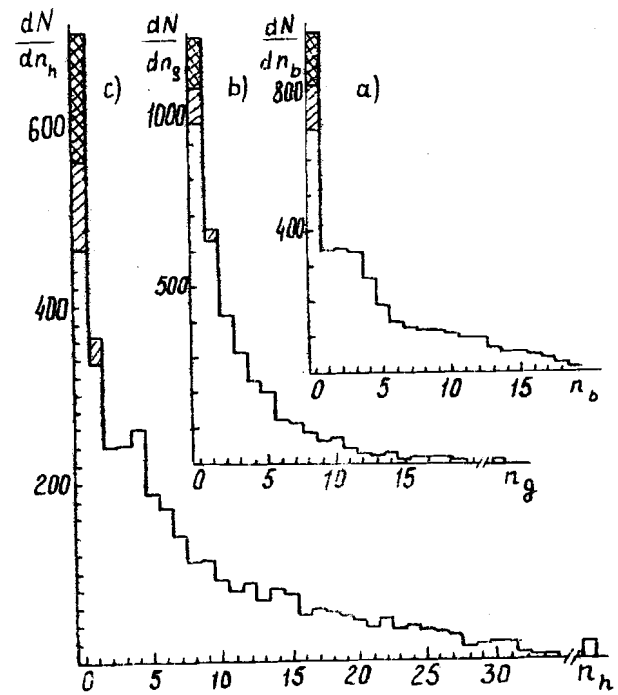

Figure 1.

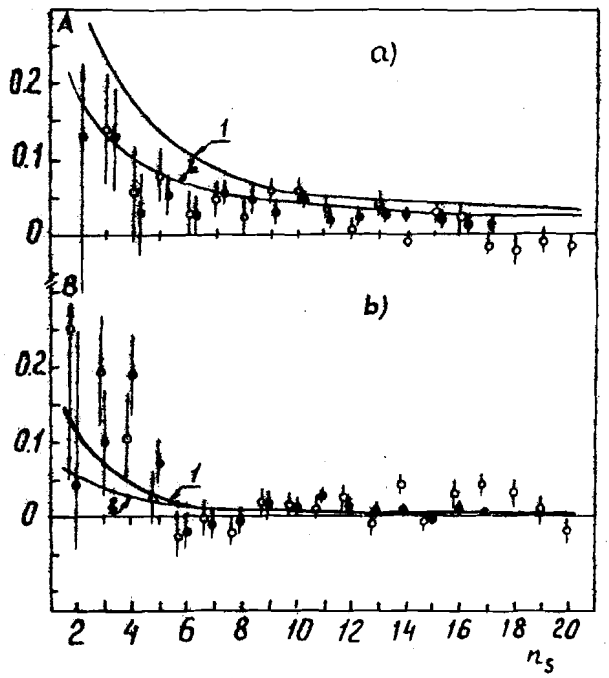

Figure 2.

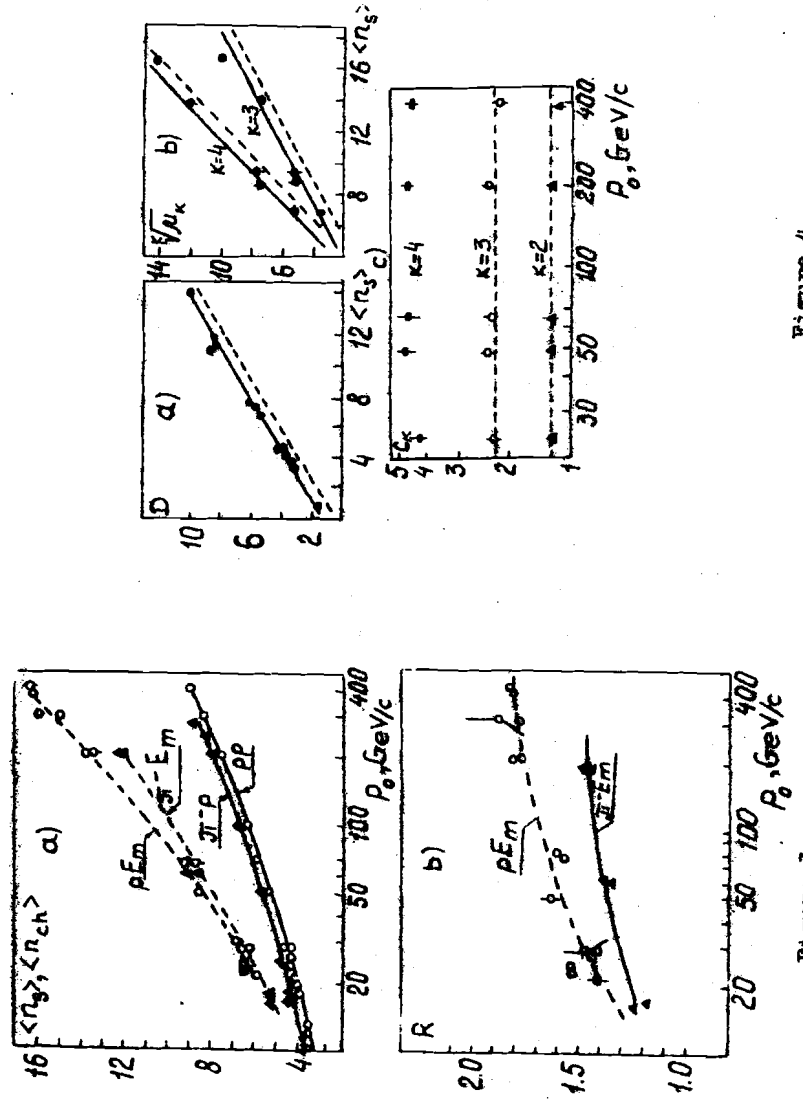

Figure 3.

Figure 4.

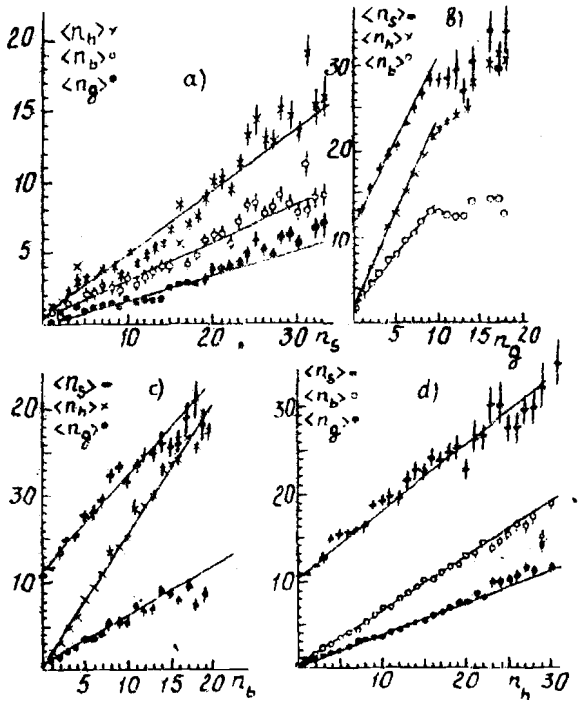

Figure 5.

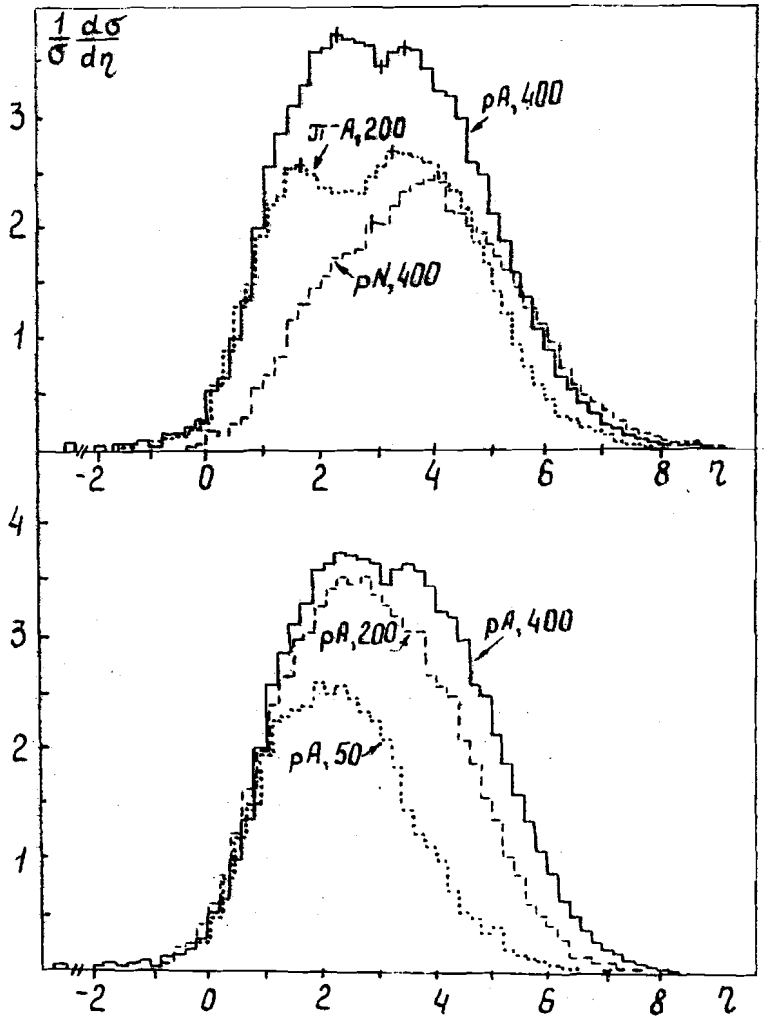

Figure 6.

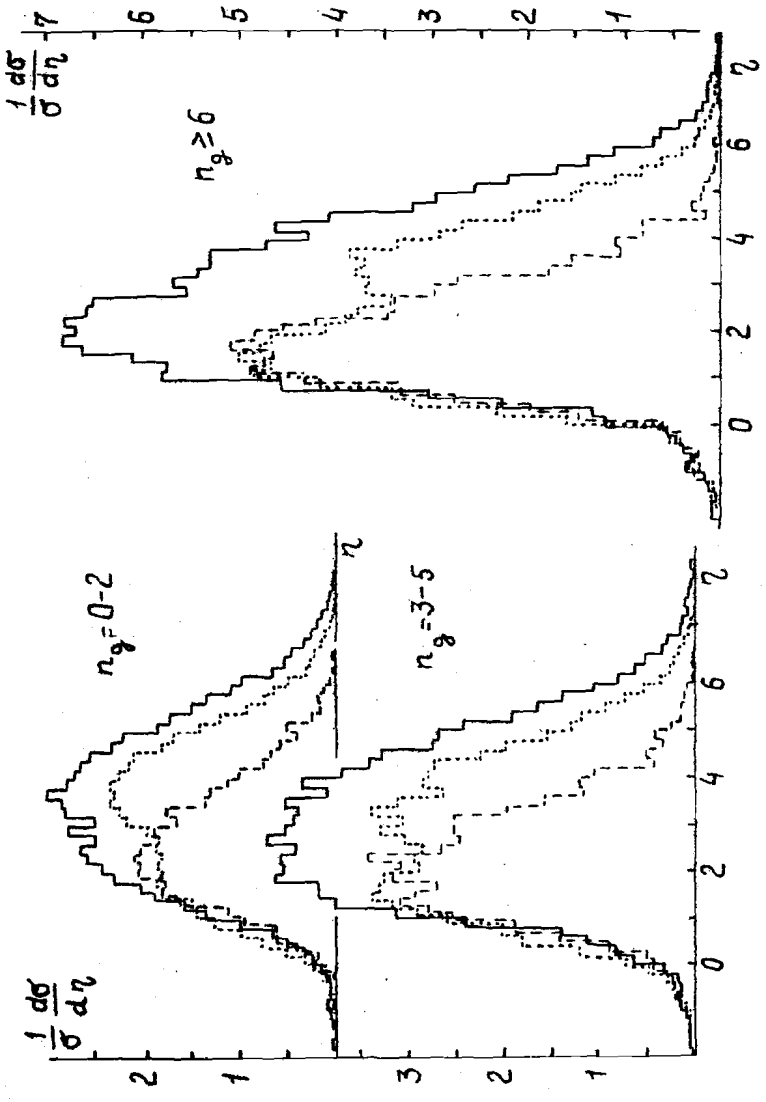

Figure 7.

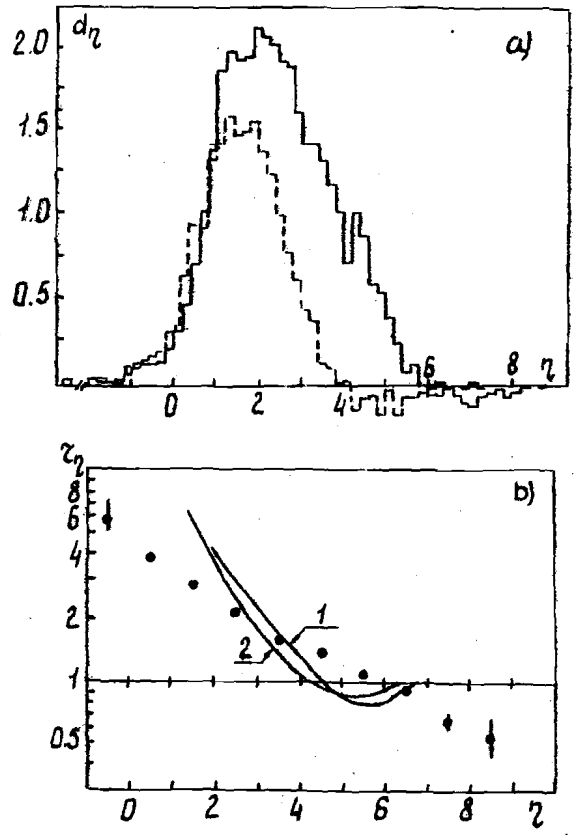

Figure 8.

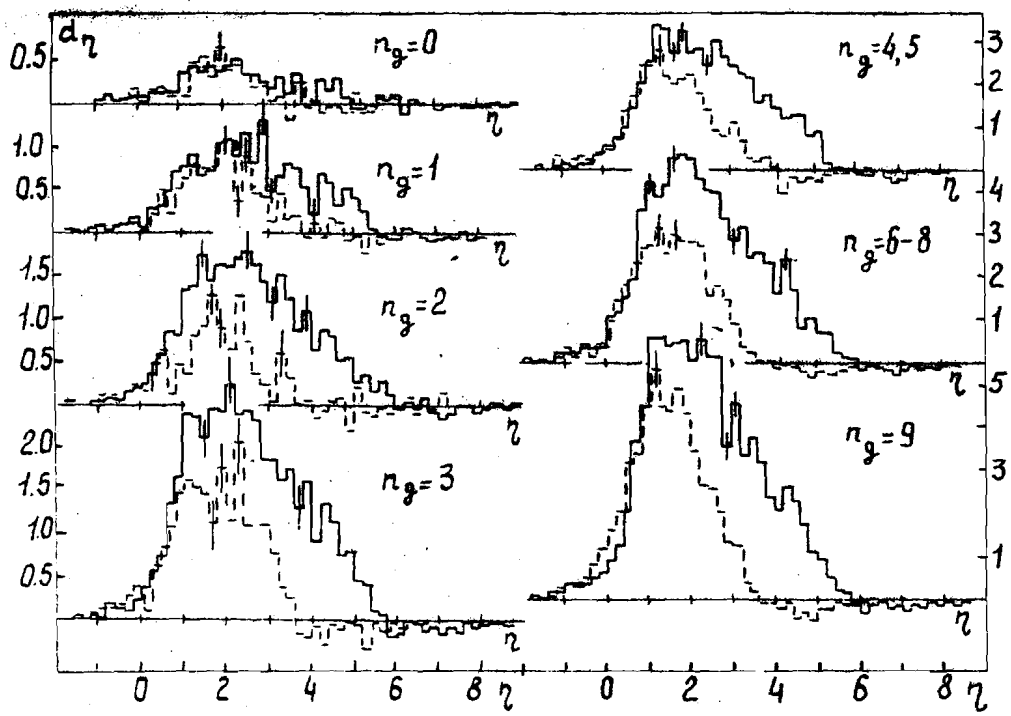

Figure 9.

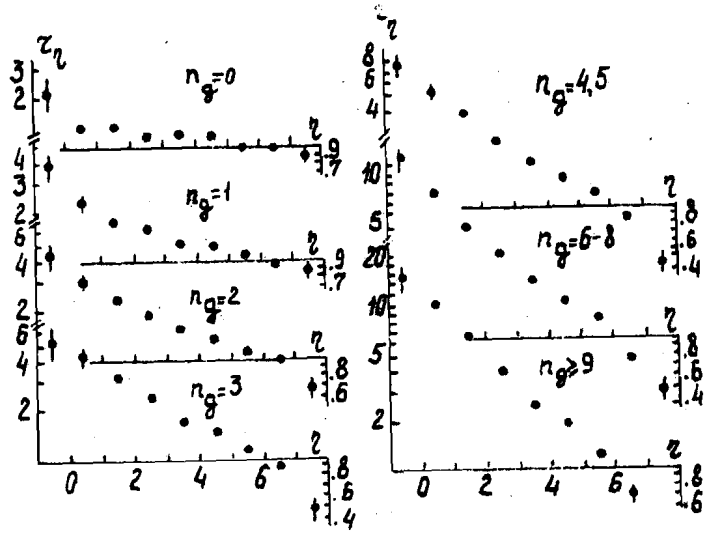

Figure 10.

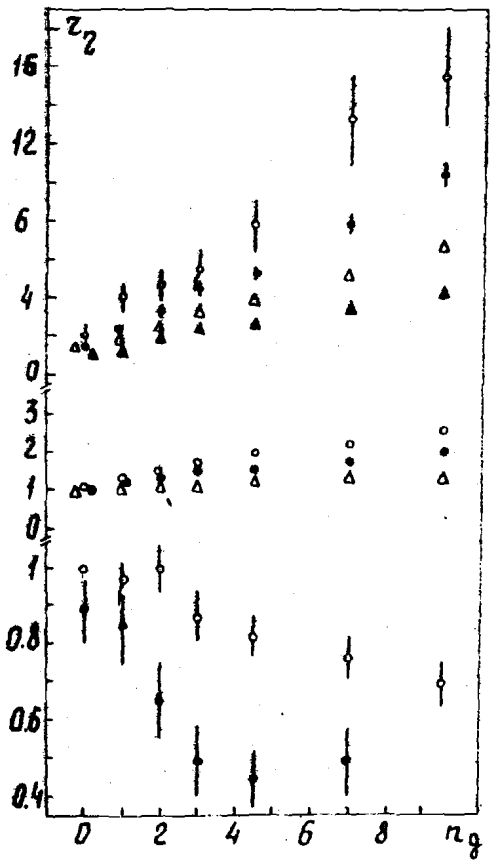

Figure 11.

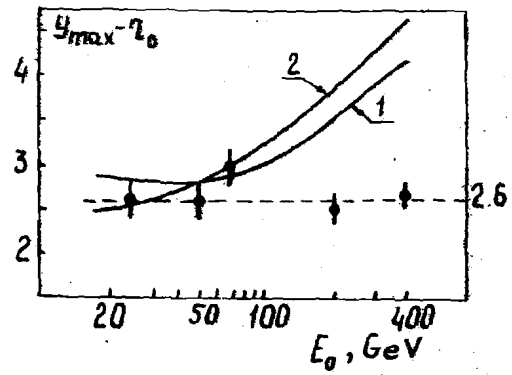

Figure 12.

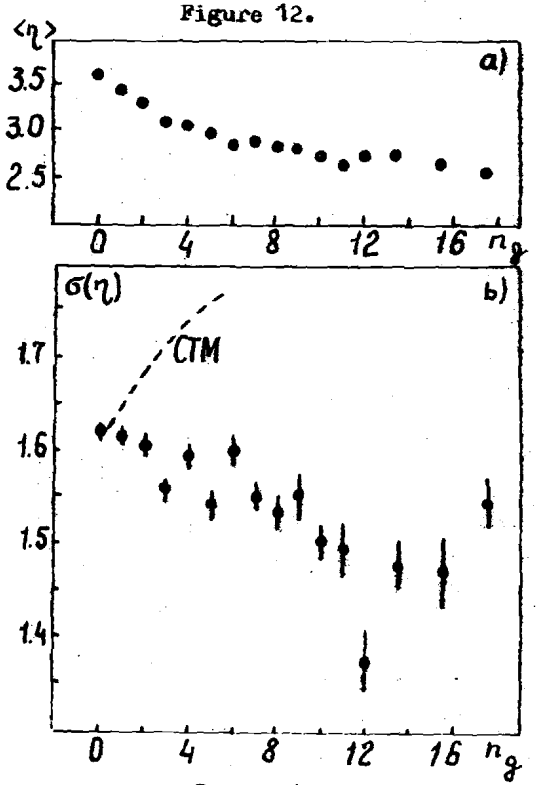

Figure 13.

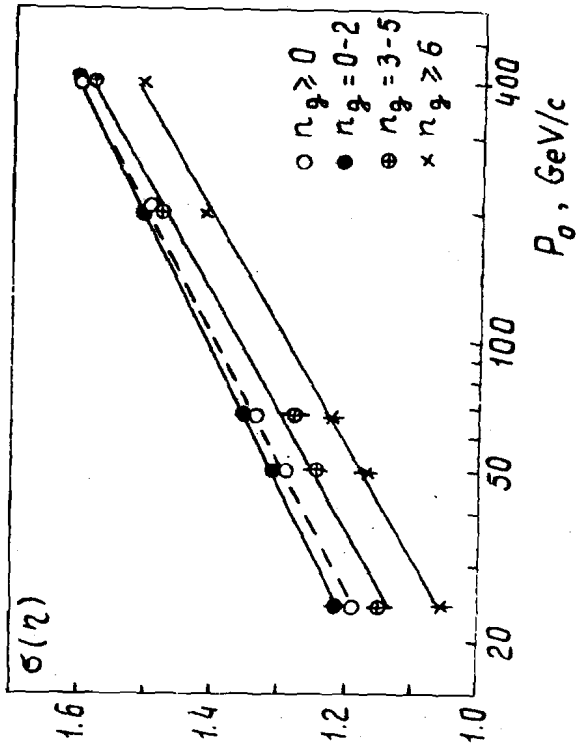

Figure 14.

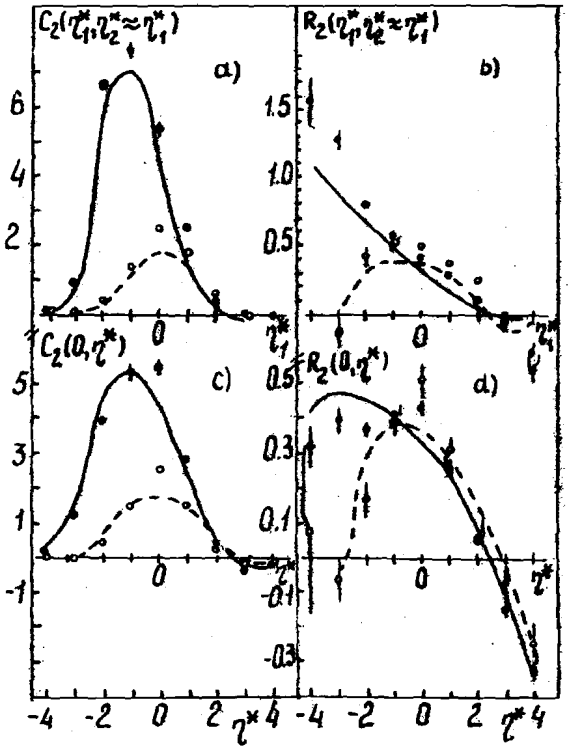

Figure 15.

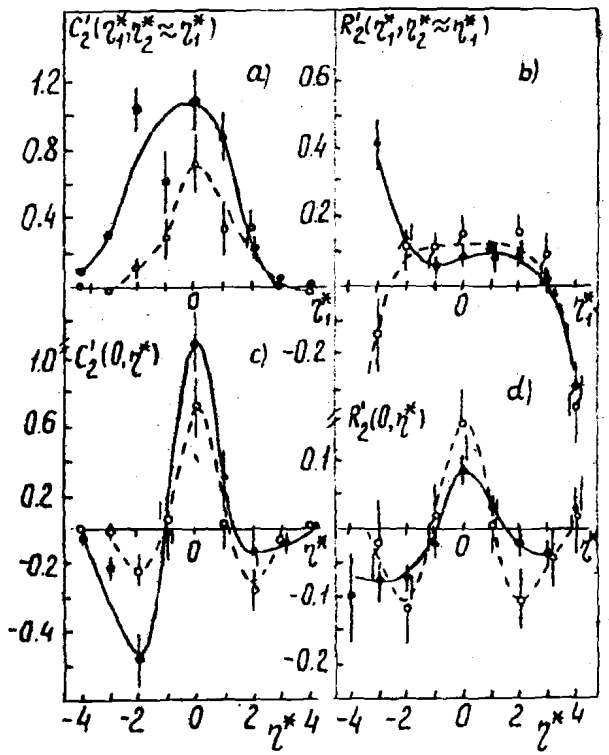

Figure 16.

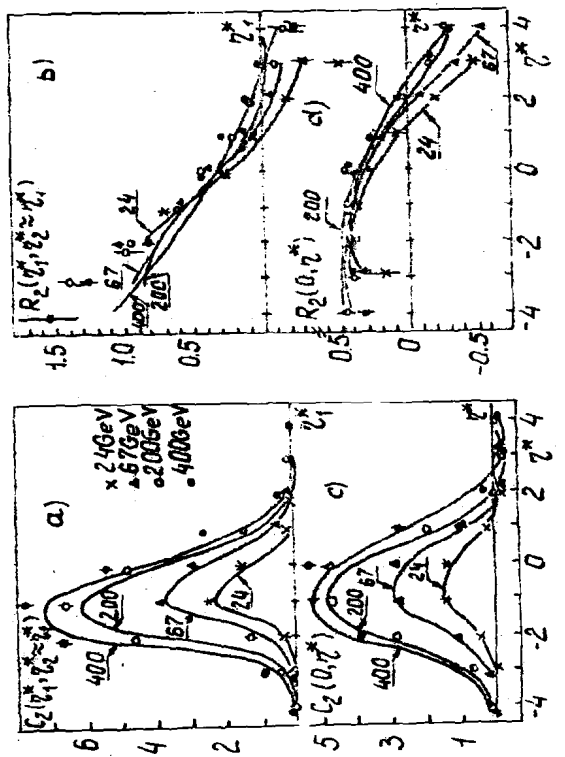

Figure 17.

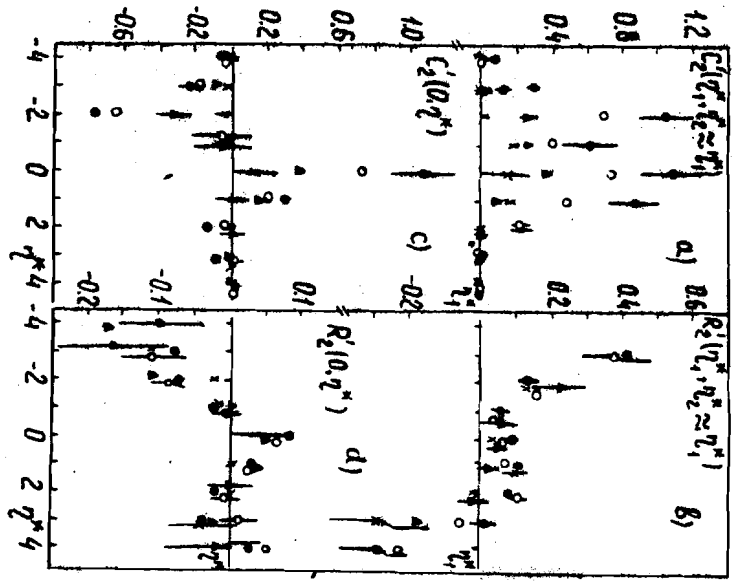

Figure 18.

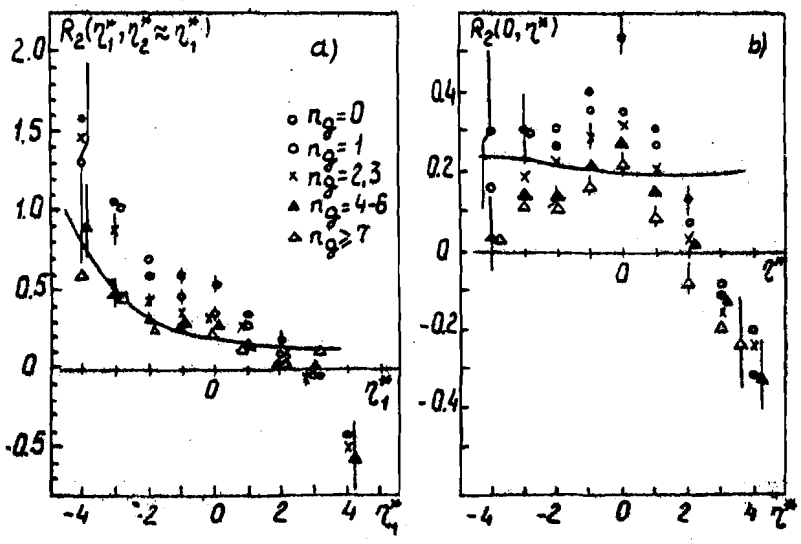

Figure 19.

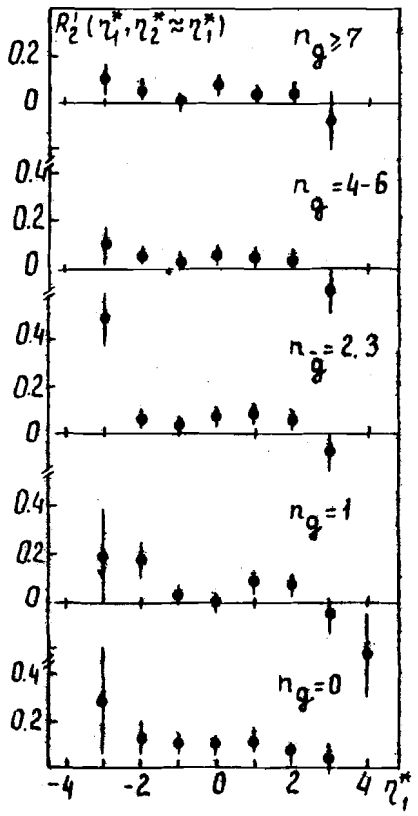

Figure 20.

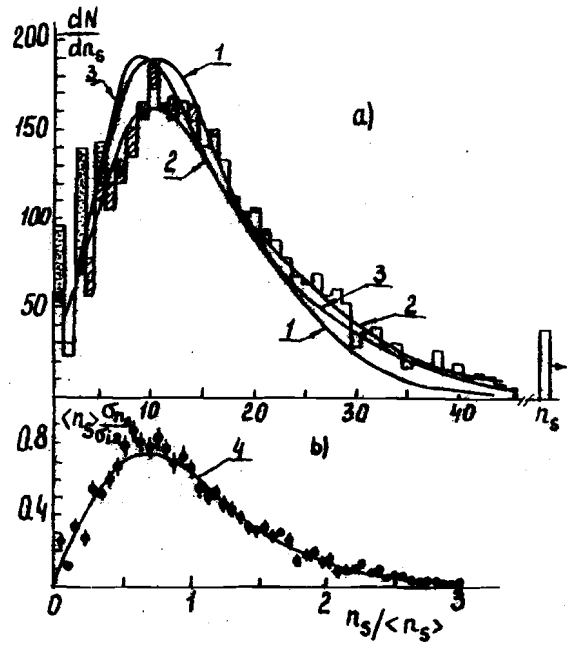

Figure 21.